

# Spin/parity of Higgs-like particle at D0

Boris Tuchming<sup>1,a</sup> for the D0 Collaboration.

<sup>1</sup>CEA Saclay - Irfu/SPP - France.

**Abstract.** We present prospects for tests of different spin and parity hypotheses for a particle  $H$  of mass 125 GeV produced in association with a vector boson and decaying into a pair of b-quarks. We use the combined analysis of the  $WH \rightarrow \ell\nu b\bar{b}$ ,  $ZH \rightarrow \ell^+\ell^-b\bar{b}$ , and  $ZH \rightarrow \nu\bar{\nu}b\bar{b}$  channels based on the full Run II dataset collected at  $\sqrt{s} = 1.96$  TeV with the D0 detector at the Fermilab Tevatron collider.

## 1 Introduction

In the standard model (SM), the electroweak symmetry breaking mechanism results from the existence of a single elementary scalar field doublet that acquires a non-zero vacuum expectation value and manifests itself as a scalar particle, the Higgs boson, the mass of which is free parameter in the model.

Finding the Higgs boson has been one of the most topical goals of particle physicists in the last decades. In summer 2012, the CDF and D0 Collaborations reported excesses above background expectations in the  $H \rightarrow b\bar{b}$  search channels [1, 2]. Their combination yields an excess at the three s.d. level, consistent with the production of a Higgs boson of mass  $M_H \approx 125$  GeV [3]. At the same time, the ATLAS and CMS Collaborations reported the discovery of a new particle at the five standard deviation (s.d.) level, consistent with the observation of a Higgs boson of  $M_H \approx 125$  GeV in the  $H \rightarrow ZZ$  and  $H \rightarrow \gamma\gamma$  channels [4, 5].

After the discovery of this new particle, comes the time to establish its properties, such as mass, spin, parity, and couplings strengths, and check if it is the Higgs boson of the SM. Testing properties in the Tevatron  $VH \rightarrow Vb\bar{b}$  modes would provide a consistent complementary information relative to the numerous spin/parity analyses performed at the LHC in the  $H \rightarrow \gamma\gamma$ ,  $H \rightarrow ZZ$ , and  $H \rightarrow W^+W^-$  modes. This proceedings discusses tests of spin/parity for the new particle of 125 GeV using the SM Higgs boson  $VH \rightarrow Vb\bar{b}$  search channels. The analysis is based on the full Run II dataset consisting of  $\sim 10$  fb<sup>-1</sup> of  $p\bar{p}$  collision recorded at  $\sqrt{s} = 1.96$  TeV with the D0 detector at Fermilab.

## 2 Principles

In general spin/parity of a particle affects angular correlations of its decay products, but also excitation curve

behavior near production threshold. For example, the cross-section for the process  $e^+e^- \rightarrow Z^* \rightarrow ZH$  at center-of-mass energy  $\sqrt{s}$  exhibits a behavior varying like  $\sigma \sim \beta = \sqrt{\frac{s-(M_H+M_Z)^2}{s-(M_H-M_Z)^2}}$  due to  $s$ -wave contributions if  $J^P(H) = 0^+$ , as for the SM Higgs boson [6]. This is modified into  $\sigma \sim \beta^3$  (due to  $p$ -wave) if  $J^P = 0^-$ . For particle with  $J^P(H) = 2^+$ , many possibilities are allowed for the  $HZZ$  coupling, but certain models end up with the cross-section dominated by the  $d$ -wave terms, resulting in a  $\sigma \sim \beta^5$  dependence.

At hadronic colliders, such as the Tevatron, the same effect is expected in the  $q\bar{q} \rightarrow VH$  process. However, the effective center of mass energy  $\sqrt{\hat{s}}$  is not fixed and depends on both cross-section dynamics and the parton density functions. Thus, the spin/parity of the particle  $H$  affects the shape of the differential cross-section as a function of effective energy,  $\sqrt{\hat{s}}$ , of the process  $p\bar{p} \rightarrow VH \rightarrow Vb\bar{b}$  [7].

This later property can be exploited in the  $VH \rightarrow Vb\bar{b}$  search modes by using discriminating variables related to the total energy: either the overall mass of reconstructed objects, or their transverse mass for final states with missing transverse energy ( $E_T$ ) due to neutrinos. The difference in shape for such observables is shown in Fig. 1. In the following we use the  $J^P = 0^+$ ,  $J^P = 0^-$ , and  $J^P(H) = 2^+$  signal models as described in [7] for particles of mass 125 GeV. The signal Monte Carlo samples are generated by the Madgraph 5 version 1.4.8.4 generator [8].

## 3 Data analysis

The data analysis follows closely the steps of the search for SM Higgs boson, in the  $WH \rightarrow \ell\nu b\bar{b}$  [9],  $ZH \rightarrow \ell^+\ell^-b\bar{b}$  [10], and  $ZH \rightarrow \nu\bar{\nu}b\bar{b}$  [11] search channels, except that in the final step, we employ the overall mass or transverse mass of the selected events as final discriminant instead of a dedicated multivariate discriminant. These analyses rely on good  $b$ -tagging efficiency, good dijet mass resolution, high- $p_T$  lepton acceptance, good modeling of

a. e-mail: tuchming@cea.fr

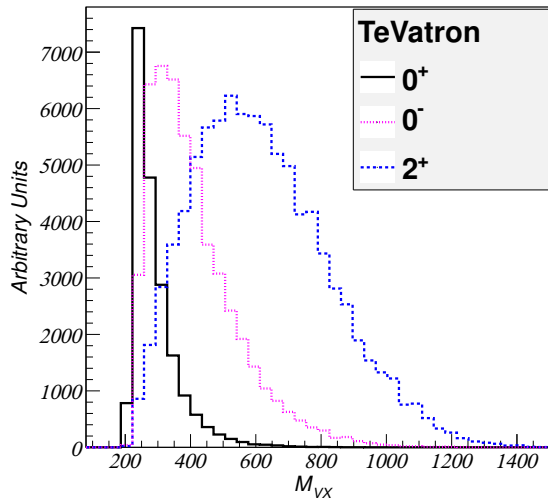


**Figure 1.** Distribution of the total invariant mass of the  $VH$  system at Tevatron for different spin/parity hypotheses (figure extracted from Ref. [7]).

the  $\cancel{E}_T$ , and good modeling of the  $V$ +jet background. The tagging of  $b$ -jets is performed with a boosted decision tree (BDT)  $b$ -tagger.

The main feature of the selections are as follows:

- The  $WH \rightarrow \ell\nu b\bar{b}$  search channel relies on the selection of isolated high- $p_T$  electrons or muons, at least two jets, and large  $\cancel{E}_T$ . A BDT discriminant is used to discriminate against multijet background. The sample of selected events is divided into exclusive subchannels according to lepton flavors and  $b$ -tagger outputs: 1 tight tag, 2 loose tag, 2 medium tag, 2 tight tag. To discriminate signal events from background events, a BDT final discriminant is constructed for each lepton flavor, jet multiplicity, and  $b$ -tagging category. In addition to kinematic variables, the inputs to the final discriminants include the  $b$ -tagger output and the output from the multijet discriminant. The BDT is trained against the SM Higgs boson signal, but its discriminating power happens to be close to optimal for  $0^-$  or  $2^+$  signal, as can be seen in Fig. 2 (bottom), where the BDT output (denoted MVA) distribution is shown for the 2-tight-tag sample.
- The  $ZH \rightarrow \ell^+\ell^-b\bar{b}$  analysis requires two isolated charged leptons of opposite charge and at least two jets. The lepton acceptance is increased thanks to secondary channels with loose lepton identification criteria: electrons in the D0 inter-cryostat region, and isolated tracks not reconstructed in the muon spectrometer. A kinematic fit corrects the measured jet energies to their best fit values according to the constraints that the dilepton invariant mass should be consistent with the  $Z$  boson mass  $M_Z$  and the total transverse momentum of the leptons and jets should be consistent with zero. A first jet is demanded to pass tight  $b$ -tagging criteria. The events are then divided into double-tag and single-tag subchannels depending on whether a second jet passes a loose

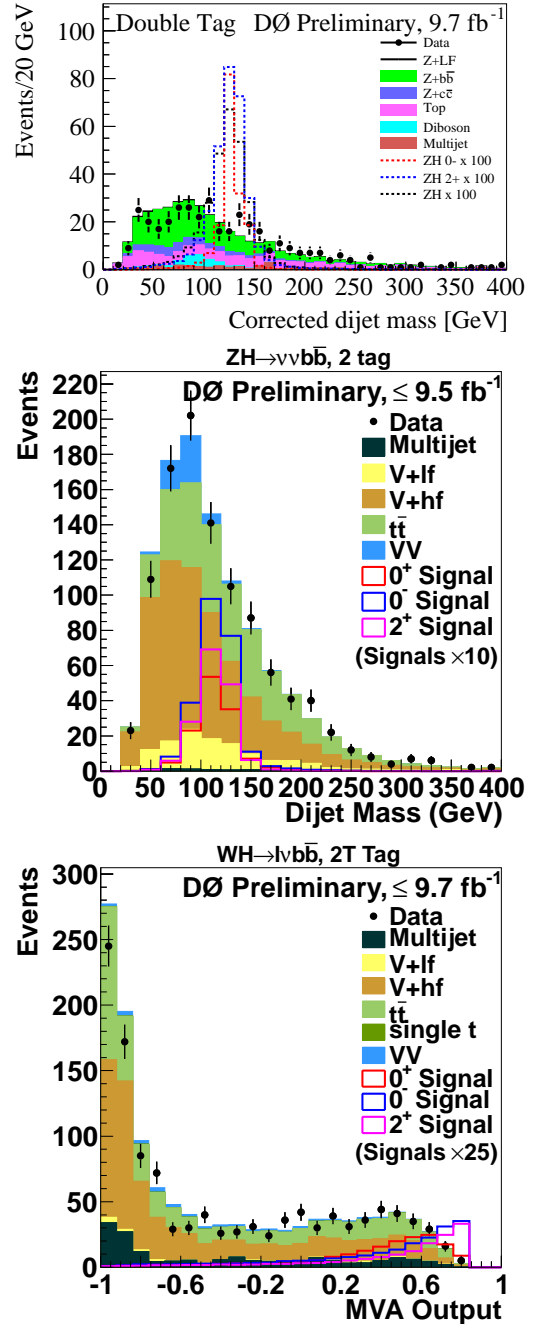


**Figure 2.** Distributions of variables employed to enhance signal over background purity, for (top) the  $ZH \rightarrow \ell^+\ell^-b\bar{b}$ , (middle)  $ZH \rightarrow \nu\nu b\bar{b}$ , and (bottom)  $WH \rightarrow \ell\nu b\bar{b}$  channels.

$b$ -tagging requirement. Figure 2 (top) presents the distribution of the dijet invariant mass for selected events in the double-tag sample.

- The  $ZH \rightarrow \nu\nu b\bar{b}$  analysis selects events with large  $\cancel{E}_T$  and two jets. This search is also sensitive to the  $WH$  process when the charged lepton from  $W \rightarrow \ell\nu$  decay is not identified. To reduce the multijet background a dedicated BDT discriminant is employed. Events are split in two  $b$ -tagging subchannels using the sum of the  $b$ -tagging discriminant outputs of the two jets. Figure 2

(middle) presents the distribution of the dijet invariant mass for selected events in the double-tag sample.

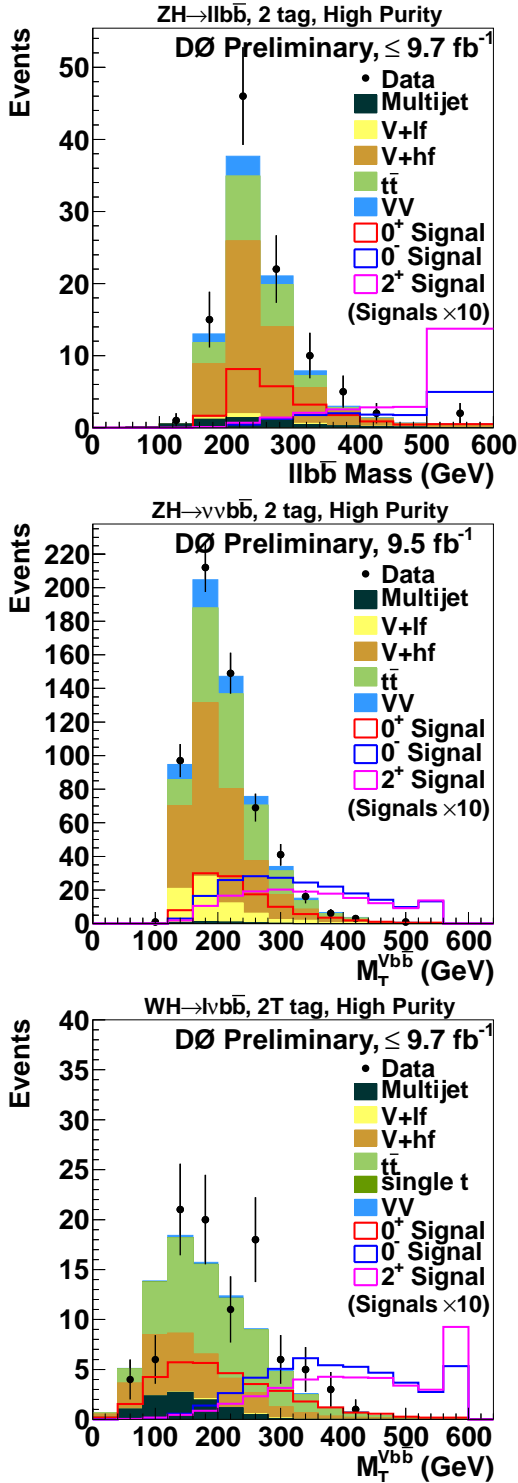


**Figure 3.** Top, Overall mass for the  $ZH \rightarrow \ell^+ \ell^- b \bar{b}$  high-purity sample at the final selection stage. Middle and bottom, overall transverse mass at the final selection stage for the high purity samples of the  $ZH \rightarrow \nu \bar{\nu} b \bar{b}$  and  $WH \rightarrow \ell \nu b \bar{b}$  channels, respectively.

To enhance the signal over background ratio at the final selection stage, the selected samples are split into higher

and lower-purity regions according to the dijet invariant mass for  $ZH \rightarrow \ell^+ \ell^- b \bar{b}$  and  $ZH \rightarrow \nu \bar{\nu} b \bar{b}$ , and the final BDT discriminant output for  $WH \rightarrow \ell \nu b \bar{b}$ . The  $WH \rightarrow \ell \nu b \bar{b}$  channel defines low-, medium-, and high-purity regions according to  $-1 < MVA \leq 0$ ,  $0 < MVA \leq 0.5$ , and  $0.5 < MVA$ , respectively. In the  $ZH \rightarrow \nu \bar{\nu} b \bar{b}$  channel, the low purity region is defined by  $M_{jj} < 70 \text{ GeV}$  or  $M_{jj} > 150 \text{ GeV}$ , and the high purity region by  $70 \leq M_{jj} \leq 150 \text{ GeV}$ . In the  $ZH \rightarrow \ell^+ \ell^- b \bar{b}$  channel, the low purity region is defined by  $M_{jj} < 100 \text{ GeV}$  or  $M_{jj} > 160 \text{ GeV}$ , and the high purity region by  $100 \leq M_{jj} \leq 160 \text{ GeV}$ .

As discussed above, the main variables to discriminate the  $2^+$  and  $0^-$  signals against the background and the  $0^+$  Higgs boson are the total dilepton+dijet mass in the  $\ell \ell b \bar{b}$  final states, and the total transverse mass for the  $\ell \nu b \bar{b}$  and  $\nu \bar{\nu} b \bar{b}$  final states. Their distributions are shown in Fig. 3.

## 4 Expected results

The final step of the analysis consists in constructing a log-likelihood ratio test-statistic  $LLR = -2 \ln(L_{H_1}/L_{H_0})$ , based on the final discriminant distributions of candidate events, where  $L_{H_0}$  is the likelihood function for the SM-Higgs-boson-plus-background hypothesis ( $0^+$ -plus-background), and  $L_{H_1}$  is either the likelihood function for the  $0^-$ -plus-background hypothesis or the  $2^+$ -plus-background hypothesis. In this test we assume that cross-sections times branching fractions are identical to the SM one. In the LLR calculation the signal and background rates are functions of the systematic uncertainties which are taken into account as nuisance parameters with Gaussian priors. Their degrading effect is reduced by fitting signal and background contributions to the data by maximizing the profile likelihood function for the  $H_0$  and  $H_1$  hypotheses separately, appropriately taking into account all correlations between the systematic uncertainties [12].

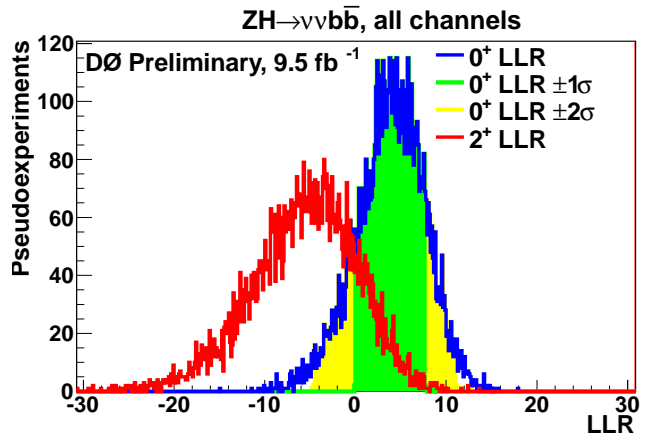


**Figure 4.** Distribution of  $LLR$  in the  $ZH \rightarrow \nu \bar{\nu} b \bar{b}$  channel for random  $0^+$ -plus-background and  $2^+$ -plus-background pseudo-experiments.

Figure 4 shows the distributions of pseudo-experiments for the  $LLR$  constructed for  $ZH \rightarrow \nu \bar{\nu} b \bar{b}$  channel only, with  $H_1$  being the  $2^+$ -plus-background

hypothesis. Two set of random pseudo-experiments have been drawn, under the  $H_1$  and  $H_0$  hypotheses, respectively. This figure demonstrate the good separation between the two hypotheses. In the SM hypothesis, the expected  $2^+$  confidence level,  $P(LLR \geq LLR^{obs} | H_1 = 2^+ \text{-plus-background})$  amounts to approximately 3.5%. Further separation is expected once the three channels will be combined.

## 5 Conclusion

The Tevatron  $VH \rightarrow Vb\bar{b}$  Higgs search channels can be used to probe the spin/parity properties of the newly discovered Higgs-like particle. The D0 Collaboration has started an analysis based on these search channels to test the  $J^P = 0^-$  and  $J^P = 2^+$  hypotheses. A good separation power between the  $J^P = 2^+$  and the SM Higgs boson ( $J^P = 0^+$ ) is demonstrated with the  $ZH \rightarrow \nu\bar{\nu}b\bar{b}$  channel only. More separation is expected once all channels will be combined. The results of this analysis are expected to be released soon.

## 6 Acknowledgments

We thank the staffs at Fermilab and collaborating institutions, and acknowledge support from the DOE and NSF (USA); CEA and CNRS/IN2P3 (France); MON, NRC KI and RFBR (Russia); CNPq, FAPERJ, FAPESP and FUNDUNESP (Brazil); DAE and DST (India); Colciencias (Colombia); CONACyT (Mexico); NRF (Korea); FOM (The Netherlands); STFC and the Royal Society (United Kingdom); MSMT and GACR (Czech Republic); BMBF and DFG (Germany); SFI (Ireland); The Swedish Research Council (Sweden); and CAS and CNSF (China).

We also thank Ken Herner who helped in the preparation of this talk.

## References

- [1] T. Aaltonen *et al.* [CDF Collaboration], Phys. Rev. Lett. **109**, 111802 (2012).
- [2] V. M. Abazov *et al.* [D0 Collaboration], Phys. Rev. Lett. **109**, 121802 (2012).
- [3] T. Aaltonen *et al.* [CDF and D0 Collaborations], Phys. Rev. Lett. **109**, 071804 (2012).
- [4] G. Aad *et al.* [ATLAS Collaboration], Phys. Lett. B **716**, 1 (2012).
- [5] S. Chatrchyan *et al.* [CMS Collaboration], Phys. Lett. B **716**, 30 (2012).
- [6] S. Y. Choi, D. J. Miller, 2, M. M. Muhlleitner and P. M. Zerwas, Phys. Lett. B **553**, 61 (2003)
- [7] J. Ellis, D. S. Hwang, V. Sanz and T. You, JHEP **1211**, 134 (2012)
- [8] J. Alwall, M. Herquet, F. Maltoni, O. Mattelaer and T. Stelzer, JHEP **1106**, 128 (2011)
- [9] V. M. Abazov *et al.* (D0 Collaboration), Phys. Rev. Lett **109**, 121804 (2012). V. M. Abazov *et al.* (D0 Collaboration), arXiv:1301.6122 (2013), accepted by Phys. Rev. D
- [10] V. M. Abazov *et al.* (D0 Collaboration), Phys. Rev. Lett **109**, 121803 (2012). V. M. Abazov *et al.* (D0 Collaboration), arXiv:1303.3276 (2013), accepted by Phys. Rev. D.
- [11] V. M. Abazov *et al.* (D0 Collaboration), Phys. Lett. B **716**, 285 (2012).
- [12] W. Fisher, FERMILAB-TM-2386-E (2006).